Common-Mode Voltage Mitigation Technique in Motor Drive Applications by Applying a Sampling-Time Adaptive Multi-Carrier PWM Method

ABRAHAM MARQUEZ ALCAIDE [1], (Member, IEEE), **HAO YAN** [2], (Member, IEEE),
XUCHEN WANG [3], (Student Member, IEEE), **JOSE I. LEON** [1,4], (Fellow, IEEE),
RAMON PORTILLO [1], (Member, IEEE), **GIAMPAOLO BUTICCHI** [3], (Senior Member, IEEE),
SERGIO VAZQUEZ [1], (Fellow, IEEE), **VITO GIUSEPPE MONOPOLI** [5], (Senior Member, IEEE),
MARCO LISERRE [6], (Fellow, IEEE), **AND LEOPOLDO G. FRANQUELO** [1,4], (Life Fellow, IEEE)

[1]Department of Electronic Engineering, Universidad de Sevilla, 41092 Sevilla, Spain
[2]School of Civil Aviation, Northwestern Polytechnical University, Xi'an 710072, China
[3]Department of Electrical and Electronic Engineering, University of Nottingham Ningbo China, Ningbo 315100, China
[4]School of Astronautics, Harbin Institute of Technology, Harbin 150001, China
[5]Department of Electrical and Information Engineering, Politecnico di Bari, 70126 Bari, Italy
[6]Chair of Power Electronics, Christian-Albrechts-Universität zu Kiel, 24118 Kiel, Germany

Corresponding author: Hao Yan (hao.yan@nwpu.edu.cn)

ABSTRACT Common-mode voltage (CMV) in electric drives causes leakage current causing consequently EMI problems, loss and reduction of their components' lifetime. Several solutions have been proposed which usually lead to higher cost because additional components are used. This paper is focused on the mitigation of the resulting CMV produced by the operation of the VSD by means of a specifically designed PWM method. The proposal is based on the analysis of the CMV harmonic spectrum using the Fourier analysis. The CMV mitigation is achieved by modifying the time-shift displacement of the carriers each sampling time considering a multi-carrier PWM technique. The resulting method has been evaluated in a down scaled experimental setup and it is easily implementable on mostly off-the-shelf mid-range micro-controller control platforms.

INDEX TERMS Harmonic analysis, pulse width modulation, motor drives.

I. INTRODUCTION

Power converters are widely used in multiple scenarios very important for the industry such as the integration of renewable energies, energy storage systems and motor-drive applications including fans, pumps, conveyor belts and electric vehicles, among others [1]. The electric variable speed drives (VSDs) in these systems are a key part in the whole power conversion system. The presence of industrial VSDs has grown in recent years replacing hydraulic and mechanic systems. This fact is mainly propitiated by the VSDs performance increase and the price reduction among others [2].

The associate editor coordinating the review of this manuscript and approving it for publication was Zhong Wu.

New technologies of power devices such as gallium nitride (GaN) or silicon carbide (SiC) are called to substitute the traditional silicon power devices in the VSDs in the near future [3]. Multilevel power converter VSDs have been developed in the last decades and the control and modulation strategies have been substantially improved [4]–[7]. However, despite of these technologies are mature enough and are already available to be used in the current energy scenario, the implementation of these solutions by the industry is still quite limited. Either due to limitations in system implementation, design requirements, power level and/or the slow implementation pace by the industry, the traditional three-phase two-level IGBT silicon-based power converter is the mainstream VSDs solution in the portfolio of the
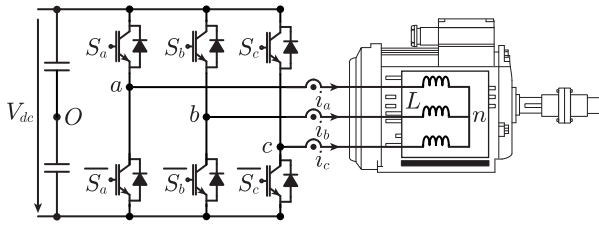
FIGURE 1. Traditional two-level three-phase inverter diagram for motor drive applications.
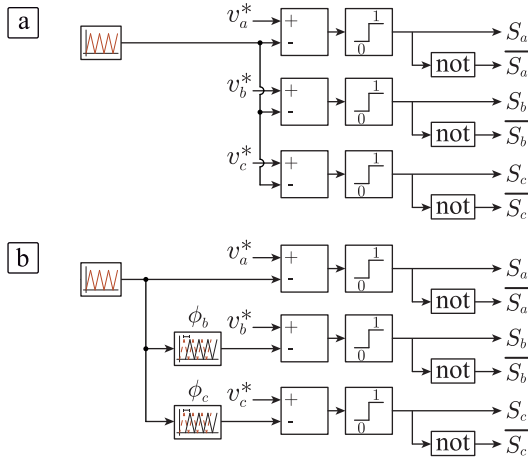

FIGURE 2. Modulation methods of the three-phase two-level converter a) Traditional single-carrier PWM method b) Proposed adaptive multi-carrier PWM technique.

FIGURE 3. Equivalent capacitance path for the leakage current in a VSD system.

industrial companies. In Fig. 1 the conventional three-phase two-level IGBT-based power converter for a motor drive application is represented.

Technical literature provides multiple well-suited strategies to control an electric VSD. Among others, it is possible to highlight the direct torque control (DTC), field oriented control (FOC) or model predictive control (MPC) techniques [5], [8]. From the converter operation point of view, the available modulation strategies to be implemented in the three-phase two-level inverter can be categorized in two main streams: space vector modulation (SVM) and carrier-based pulse-width modulation (CB-PWM) techniques [4]. Compared with the SVM method, the CB-PWM technique is the simplest and the most straightforward way to operate a power converter because most of available control platforms include specific hardware to directly implement this modulation technique. In Fig. 2a, the traditional CB-PWM method of a three-phase two-level power converter is shown.

In any case (applying the SVM or CB-PWM methods), the use of a high switching frequency in the VSD leads to many advantages such as the increase of the power density, weight reduction as well as the improvement of the machine controllability because the control of the desired currents and magnetic flux in the machine can be accurately achieved [9]. Despite of these advantages, some drawbacks related with the high-switching frequency affect directly to
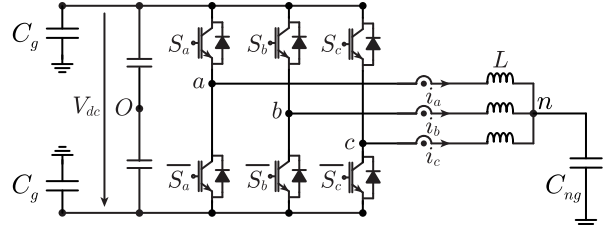
the performance and reliability of the system [10]–[12]. As an example, a conducted and radiated electromagnetic interference (EMI) appears. In addition, shaft voltage and bearing currents phenomena appear in the induction machines operation [13]–[17].

II. THE IMPORTANCE OF THE COMMON-MODE VOLTAGE IN MOTOR DRIVE APPLICATIONS

One very important issue in motor drive applications is the common-mode voltage (CMV) that is defined as the voltage present between neutral terminal in the load (n) and the middle point of the dc-link (O) represented in Fig. 3. The CMV generated by the VSD directly affects to the reliability of the motor. It has been demonstrated that the CMV is the responsible of the bearing degradation representing more than 50% of the motor failures [10], [11], [18], [19]. Different mathematical models have been developed in order to estimate an early failure of these motor components [20]–[23].

The CMV in the three-phase motor drive system causes leakage current to the ground. As illustrated in Fig. 3, C_g is the stray capacitance of the path from the dc-link to ground, which becomes a leakage current path. Besides, since there is parasitic capacitance in the motor neutral point to ground, denoted as C_{ng}, the leakage current flows through the motor frame to ground [24].

In the motor drive application, such a leakage current causes additional harmonics and energy loss in the system. Besides, it introduces electromagnetic interference and even electrical safety issues. For example, the high frequency leakage current may lead to the misoperation of the relay to ground, which is harmful to the motor drive system. The PWM inverters used in motor drive applications also introduce a CMV from the three-phase winding neutral point to ground, and a leakage current flows through parasitic capacitance between stator winding and the motor frame to the ground [25].

It is essential to reduce the CMV in the three-phase motor drive to increase its lifetime and reliability. In this sense, many advances have been performed and multiple solutions can be found in the literature which are summarized in two main categories: the introduction of external elements, and the CMV mitigation via introducing a specific control or modulation strategy. Among the solutions based on the introduction of external elements, the use of

filtering techniques and active canceler circuits are very popular [17], [26]–[31]. Although good enough results are obtained, the introduction of extra passive elements and/or new power devices with their ancillary systems and drivers is required. Therefore, the cost of the whole system, its complexity, volume and weight are increased. To the contrary, the CMV reduction via the usage of a proper modulation technique is an attractive solution being studied by the academia and industry. As an example, the switching pattern selection method in SVM has been investigated [18], [28], [30], [32]–[34]. Considering CB-PWM techniques, the available literature also provide some solutions [35], [36]. For instance, in [35], a tri-carrier PWM technique with fixed displacement angles between the carriers equal to [0°, 120°, 240°] is proposed based on empirical observation.

This paper is focused on the mitigation of the resulting CMV via the modification of the displacement angles of the carriers in a tri-carrier PWM technique during the operation of the VSD. The work develops the analysis of the generated CMV harmonic spectrum. As a consequence of this analysis, the sampling-time adaptive multi-carrier PWM technique shown in Fig. 2b is proposed. In this way, the CMV mitigation is achieved without the use of external active elements and passive filtering techniques.

III. TIME VARIANT COMMON-MODE VOLTAGE HARMONIC DESCRIPTION IN A TWO-LEVEL INVERTER

It is well-known that the CMV is determined by the summation of the phase voltages divided by the number of phases of the VSD. Therefore, considering a three-phase system, the CMV is determined as

$$\text{CMV} = \frac{V_{aO} + V_{bO} + V_{cO}}{3} \tag{1}$$

where V_{xO} is the phase voltage of phase x ($x = a, b, c$). In order to obtain the analytical expression of the CMV in a three-phase two-level VSD, the Fourier expansion series is considered:

$$x(t) = \frac{A_0}{2} + \sum_{n=1}^{\infty} \left[A_n \cos(n\omega t) + B_n \sin(n\omega t) \right] \tag{2}$$

where $\frac{A_0}{2}$ is the dc component, and A_n and B_n are the n-th harmonic order Fourier coefficients.

Figure 4 shows, as an example, a phase voltage generated by the three-phase two-level VSD when the switching signals are generated using the traditional single-carrier PWM method shown in Fig. 2, where a single triangular carrier signal with frequency f_c is used. As it is observed in Fig. 4a, the obtained phase voltage can be described as a square pulses trend which depends on the normalized voltage reference (also called duty cycle) shown in Fig. 4b. Additionally, as shown in Fig. 4c, choosing carefully the time origin (t'), each single pulse presents an odd symmetry and the coefficients of the Fourier expansion series are greatly simplified
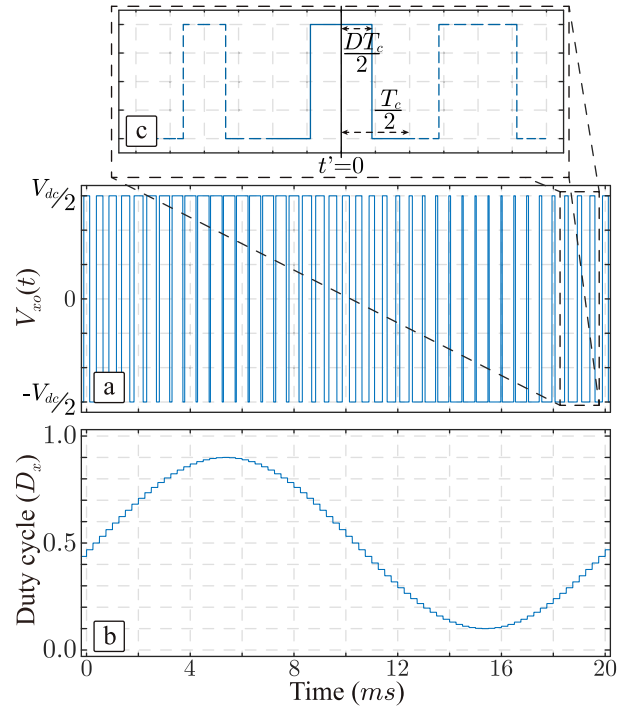

FIGURE 4. a) A fundamental period of the VSD phase voltage. b) VSD duty cycle. c) A detail of the resulting phase voltage.

because B_n coefficients are zero, leading to

$$A_{x0} = \frac{4}{T_c} \int_0^{\frac{T_c}{2}} v_{xO}(t)dt = V_{dc}(2D_x - 1)$$

$$A_{xn} = \frac{2}{T_c} \int_0^{\frac{T_c}{2}} v_{xO}(t) \cos(n\omega_c t)dt$$

$$= \frac{2V_{dc}}{T_c} \left[\int_0^{\frac{D_x T_c}{2}} \cos(n\omega_c t)dt - \int_{\frac{D_x T_c}{2}}^{\frac{T_c}{2}} \cos(n\omega_c t)dt \right]$$

$$= \frac{4V_{dc}}{n\pi} \sin(n\pi D_x) \tag{3}$$

where A_{xn} are the Fourier coefficients of the phase voltage V_{xO} and $\omega_c = \frac{2\pi}{T_c}$. In addition, as shown in Fig. 4b, D_x is the duty cycle defined as the normalized phase voltage of phase x between 0 and 1 as follows:

$$D_x = \frac{V_{xO}}{2V_{dc}} + 0.5 \tag{4}$$

Summarizing, considering the traditional single-carrier PWM approach, the phase voltages in a VSD can be described as:

$$V_{xO}(t) = V_{dc}(2D_x - 1) + \sum_{n=1}^{\infty} \frac{4V_{dc}}{n\pi} \sin(n\pi D_x) \cos(n\omega_c t) \tag{5}$$

In order to introduce the adaptive multi-carrier PWM approach that considers a different triangular carrier signal per phase, it is necessary to add the displacement angle term
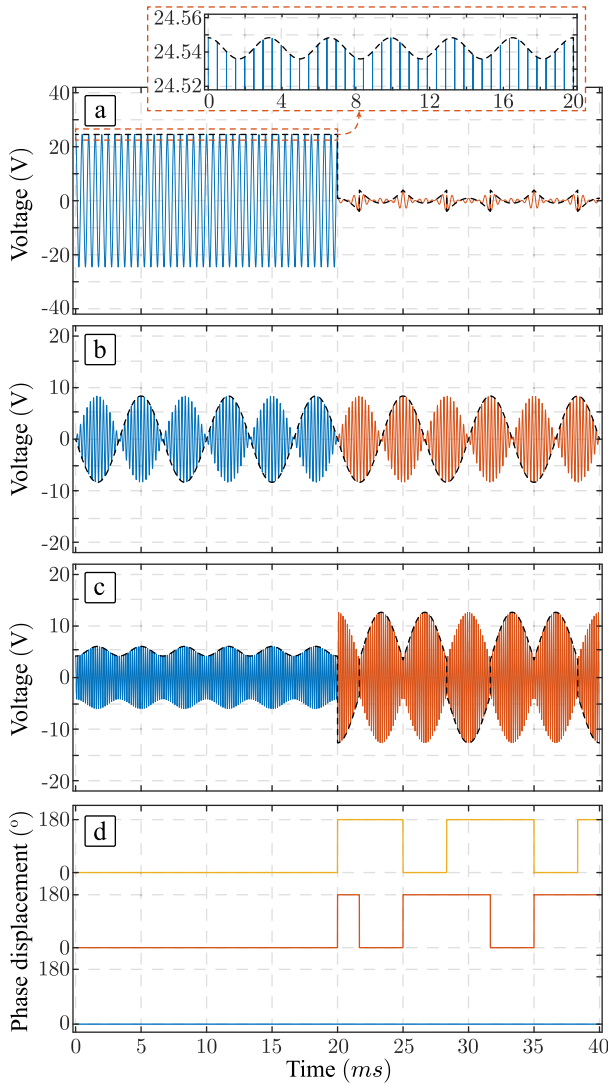
FIGURE 5. a) $CMV\rfloor_1(t)$ b) $CMV\rfloor_2(t)$ c) $CMV\rfloor_3(t)$ d) Carrier displacement angles ϕ_b and ϕ_c.

between the carriers in (5) as:

$$V_{xO}(t) = V_{dc}(2D_x - 1)$$
$$+ \sum_{n=1}^{\infty} \frac{4V_{dc}}{n\pi} \sin(n\pi D_x) \cos(n\omega_c t - n\phi_x) \quad (6)$$

where ϕ_x is the displacement angle of the carrier associated to phase x. In this way, the time description of harmonic n-th in the phase voltage V_{xO} can be described as:

$$V_{xO}\rfloor_n(t) = \frac{4V_{dc}}{n\pi} \sin(n\pi D_x) \cos(n\omega_c t - n\phi_x) \quad (7)$$

Therefore, substituting (7) into (1), each harmonic component of the CMV is determined. Each individual n-th order harmonic expression of the CMV, $CMV\rfloor_n(t)$ $(n \geq 1)$, can be evaluated as the addition of the corresponding components in the phase voltages V_{xO} by decoupling the term $\cos(n\omega_c t - n\phi_x)$ using the well-known trigonometric formula related to
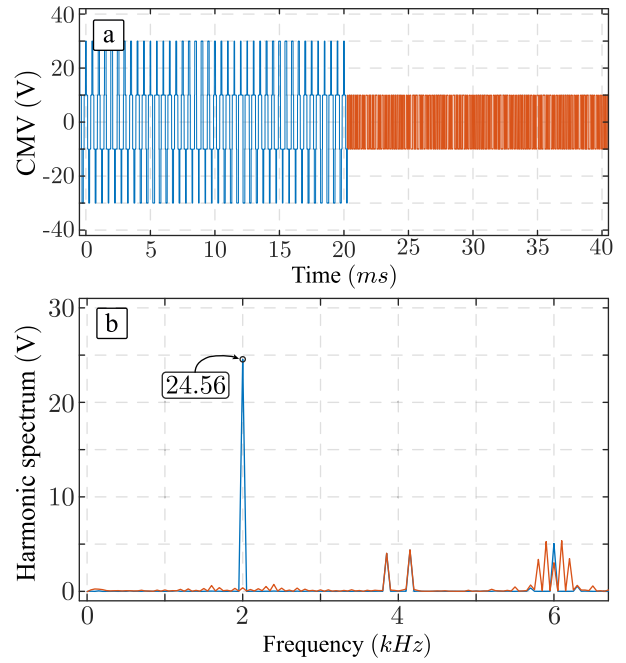

FIGURE 6. a) CMV b) Harmonic spectrum of the CMV.

$\cos(a + b)$ and considering $\phi_a = 0°$ as reference:

$$CMV\rfloor_n(t) = \frac{1}{3} \sum_{x=a,b,c} V_{xO}\rfloor_n(t)$$

$$= \frac{\cos(n\omega_c t)}{3} \Big[A_{an} + A_{bn} \cos(n\phi_b) + A_{cn} \cos(n\phi_c) \Big] \quad (8a)$$

$$+ \frac{\sin(n\omega_c t)}{3} \Big[A_{bn} \sin(n\phi_b) + A_{cn} \sin(n\phi_c) \Big] \quad (8b)$$

IV. CMV MITIGATION USING A SAMPLING-TIME ADAPTIVE TRI-CARRIER PWM METHOD

As shown in section III, $CMV\rfloor_n(t)$ is highly dependent on the values of the displacement angles of the carriers ϕ_b and ϕ_c. To illustrate this fact, a test has been done and the simulation results are presented in Fig. 5 and Fig. 6. Initially, from $t = 0$ to $t = 20$ms, it is considered the conventional single-carrier PWM strategy shown in Fig. 2 with $f_c = 2$kHz where $\phi_a = \phi_b = \phi_c = 0°$. The resulting $CMV\rfloor_n(t)$ waveform signals are represented in Fig. 5 whereas the resulting total CMV and its harmonic spectrum are represented in Fig. 6, colored in blue. It can be observed that the CMV harmonic spectrum presents a high amplitude in the first $(n = 1)$ harmonic component (2kHz).

As it is observed in Fig. 5, each single harmonic component $CMV\rfloor_n(t)$ presents a high similarity with the amplitude modulation technique widely used in the radio transmission field since decades. Analyzing both equations and comparing with the amplitude modulation technique, the magnitudes inside square brackets in (8a) and (8b) act as modulating signals and therefore, modifying their amplitudes it is possible to mitigate the harmonic content of the resulting CMV.
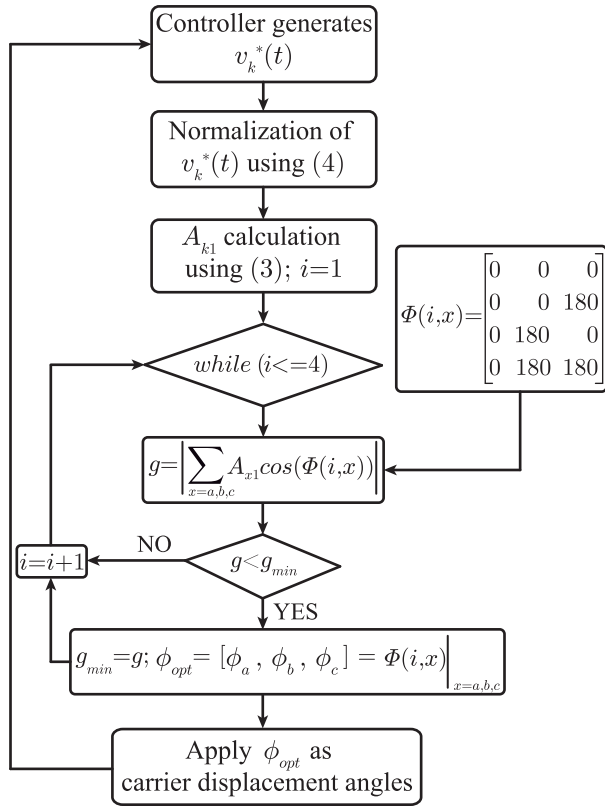
FIGURE 7. Sampling-time algorithm flowchart to determine the displacement angles of the carriers to achieve the mitigation of the first harmonic order content in the CMV.
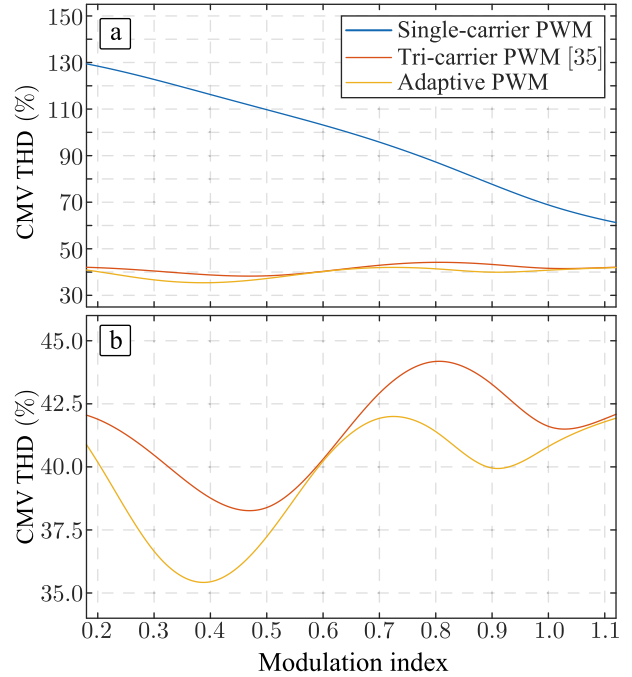

FIGURE 8. CMV THD in a modulation index range from 0.2 to 1.1 a) considering the three PWM methods b) zoom of the results obtained using the tri-carrier PWM methods.

In essence, the mitigation of the CMV component of n-th order is based on solving the following system of equations:

$$A_{an} + A_{bn}\cos(n\phi_b) + A_{cn}\cos(n\phi_c) = 0$$
$$A_{bn}\sin(n\phi_b) + A_{cn}\sin(n\phi_c) = 0 \qquad (9)$$

The analytical solution of (9) has been already provided by the academia [37], [38]. However, due to the nature of the problem and the formulation of the coefficients, it can be proven that the analytical expression does not always provide a valid solution into the set of real numbers and therefore, a single harmonic cancellation can not be assured.

According with the mathematical formulation in (9), a CMV harmonic mitigation can be achieved by the clever determination of the ϕ_b and ϕ_c carrier displacements. The proposed adaptive multi-carrier PWM method considers the carrier phase displacement $\phi_a = 0°$, while the angles ϕ_b and ϕ_c, for the sake of simplicity, only take values equal to $0°$ or $180°$. Under this assumption, (8b) remains always zero. In this way, the final values of ϕ_b and ϕ_c ($0°$ or $180°$) in order to minimize $CMV\rfloor_n(t)$ are those that will minimize (in absolute value) the mathematical term introduced in (8a). In the proposed method, each sampling time, the term (8a) is evaluated with the existing four possible values of $[\phi_b, \phi_c]$ which are $[0°, 0°]$, $[180°, 0°]$, $[0°, 180°]$ and $[180°, 180°]$. Once the four possibilities are evaluated, the most convenient solution is implemented. A flowchart of the calculations required to

determine the displacement angles of the carriers to mitigate the content of the first harmonic order content of the CMV ($CMV\rfloor_1(t)$) is illustrated in Fig. 7. It is worth to mention that trigonometric functions can be pre-calculated since the cosines of $0°$ and $180°$ degrees are well-known values. In this sense, the computational burden is not increased significantly.

The simulation results applying the proposed sampling-time adaptive multi-carrier PWM method are represented in Fig. 5 and Fig. 6 from $t = 20$ ms (drawn in red). It can be observed that $CMV\rfloor_1(t)$ (which is the dominant harmonic component) is practically eliminated without a significant increase of the second and the third CMV harmonic groups.

The proposed adaptive multi-carrier PWM approach has been tested considering a modulation index range from 0.2 to 1.1. A comparison in terms of the CMV total harmonic distortion (THD) considering the traditional single-carrier PWM method as well as the tri-carrier PWM method with fixed displacement angles of the carriers equal to $[\phi_a, \phi_b, \phi_c]=[0°, 120°, 240°]$ (proposed in [35]) is shown in Fig. 8. As it can be observed, the proposed sampling-time adaptive multi-carrier PWM technique significantly reduces the CMV THD produced by the traditional single-carrier PWM method and also improves the performance given by the tri-carrier PWM with fixed displacement angles.

The harmonic improvement achieved by the proposed adaptive modulation technique can be proven if [35] is analyzed in detail. The fixed angle displacement proposed in [35] effectively eliminates the harmonic component located in $[m = 1, n = 0]$ (following the notation used in the Double Fourier Integral where m defines the harmonic group and n
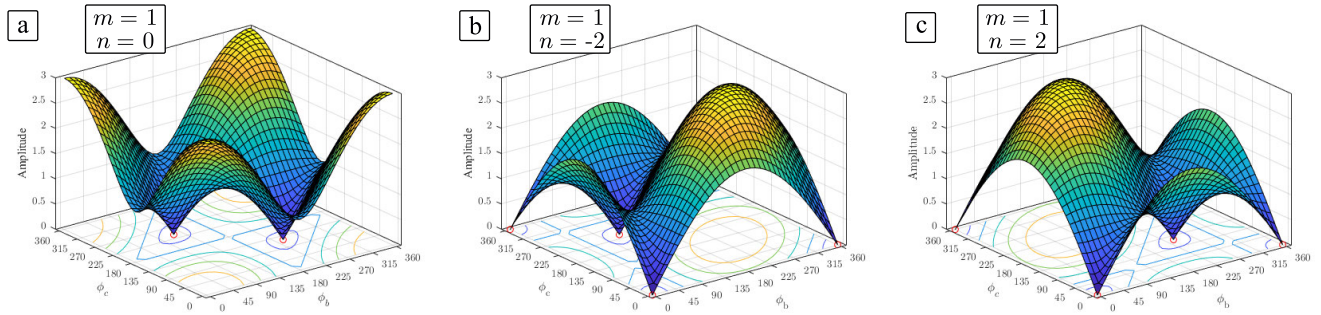
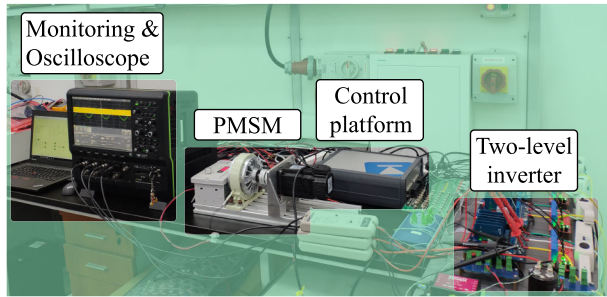**FIGURE 9.** Evaluation of the harmonic components of the first group using the tri-carrier modulation.

FIGURE 10. Down-scaled 750W three-phase PMSM laboratory prototype.

FIGURE 11. Controller scheme implemented in the experimental setup.

TABLE 1. Three-phase PMSM parameters.

Parameters	Values
Winding resistance $[\Omega]$	0.901
Winding inductance $[mH]$	6.552
Back-EMF coefficient K_E $[V/rpm]$	0.0227
Moment of inertia J $[g/m^2]$	0.12
Pole pair number	4
Voltage $[V]$	220
Nominal torque $[Nm]$	2.4
Nominal speed $[rpm]$	3000

denotes the specific harmonic position in the group). However, the harmonic components located at [$m = 1$, $n = \pm 2$] achieve their maximum values depending on the solution set chosen ($[0°, 120°, 240°]$ or $[0°, 240°, 120°]$). This effect is clearly illustrated in Fig. 9 where those three amplitudes of the harmonic components have been represented for all possible ϕ_a and ϕ_b combinations. The proposed adaptive modulation technique is based on the harmonic mitigation of the whole group since the reduction is performed in the time variant amplitude of the modulating signal which determines the harmonic components of the complete group ($m = 1$ independently of the value of n).

V. EXPERIMENTAL RESULTS

In order to test the proposed multi-carrier PWM technique and to validate the effectiveness of the analysis, the down-scaled experimental setup shown in Fig. 10 has been used. It is based on a conventional silicon IGBT three-phase two-level inverter tied to a 750 W three-phase permanent magnet synchronous machine (PMSM). The PMSM parameters are listed in Table 1.

The PMSM control and modulation strategies are implemented using the rapid prototyping real-time platform PLECS RT box [39]. Figure 11 illustrates the implemented PMSM control and modulation strategy. From the control strategy point of view, the PMSM is driven considering the traditional FOC [40]. In the modulation stage, the conventional single-carrier PWM method, the tri-carrier PWM technique with fixed carrier displacement angles [35] as well as the proposed sampling-time adaptive multi-carrier PWM
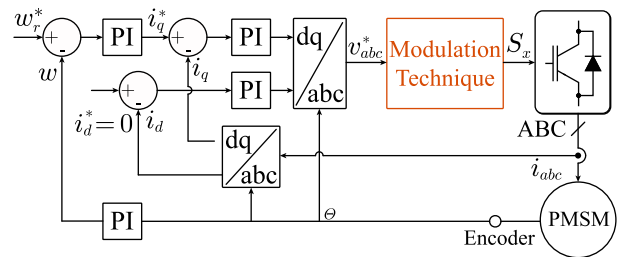
technique have been implemented in order to evaluate the obtained CMV of the power system.

In the experiments, f_c = 5kHz, the speed reference is equal to 600rpm and the dc-link voltage is 60V. As the experimental setup has not the capacitor dc-link split-off in two parts, the measurement of CMV has been taken respect to the negative pole. In this sense, the CMV THD values contain a half dc-link voltage mean value. The experimental results are summarized in Fig. 12. The resulting CMV when the conventional single-carrier PWM technique is represented in Fig. 12a and its harmonic spectrum is presented in Fig. 12b. As expected, a non-negligible harmonic distortion is located at the carrier frequency (5kHz) and its multiples.

On the other hand, the tri-carrier PWM method with fixed carrier displacement angles and the proposed sampling-time tri-carrier PWM technique with adaptive carrier displacement angles have been also evaluated. Their corresponding CMV
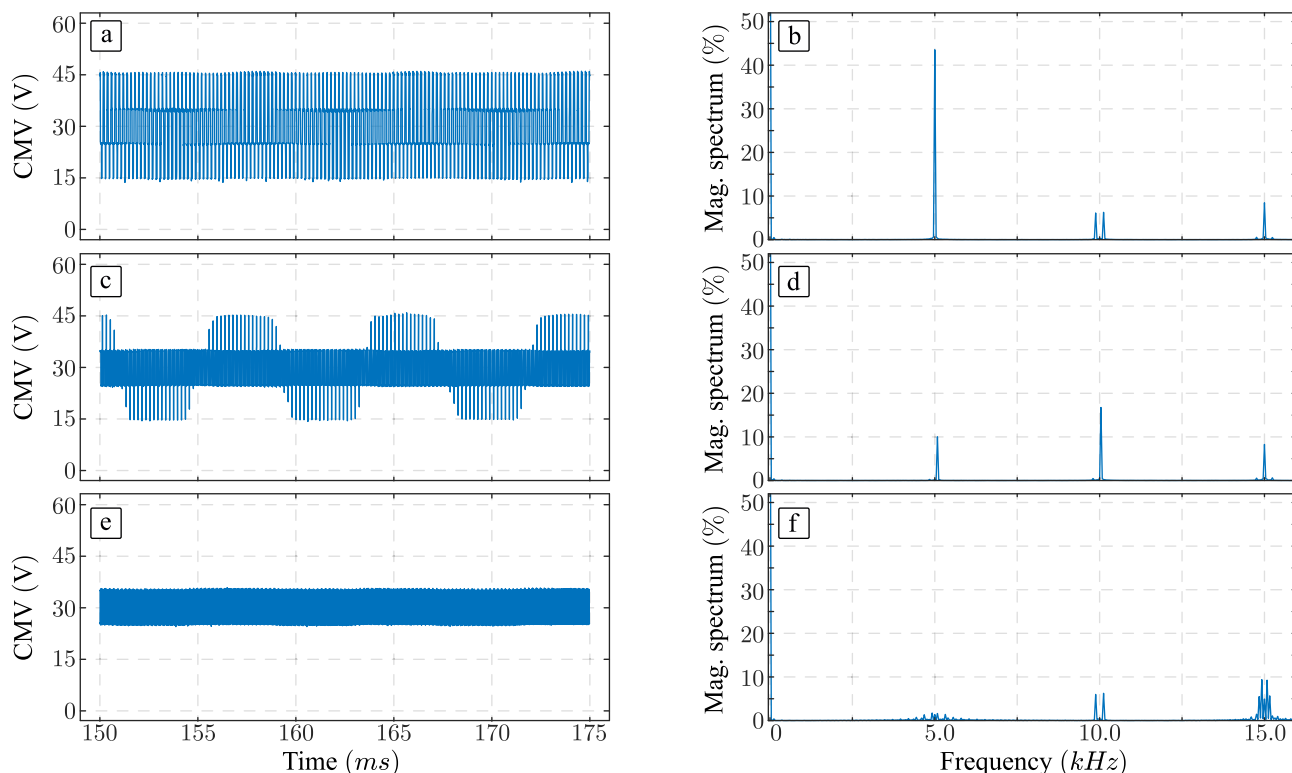
FIGURE 12. CMV generated in the PMSM (left) and CMV harmonic spectrum (right) using a) and b) the traditional single-carrier PWM method c) and d) the tri-carrier PWM [35] e) and f) CMV the adaptive multi-carrier PWM technique.

waveforms are represented in Fig. 12c and Fig. 12e, respectively. Applying the proposed PWM method, a clear reduction in the CMV peak-to-peak value can be observed. Taking a look of the resulting CMV harmonic spectrum (drawn in Fig. 12d and Fig. 12f), applying the tri-carrier PWM methods the harmonic component of the CMV located at switching frequency has been considerably reduced without a significant increase of distortion at higher frequencies. As mentioned in section IV, although the conventional tri-carrier PWM method presented in [35] effectively eliminates the dominant harmonic component located at carrier frequency ($m = 1$, $n = 0$) a new non-negligible magnitude harmonic component appears in the resulting CMV spectrum ($m = 1$ $n = \pm 2$, depending on the chosen carrier phase-displacement solution set). In addition, the magnitude of the harmonic component in the second group ($m = 2$) also increases. However, as the proposed adaptive multi-carrier PWM modulation acts over the modulating signal which determines the magnitude of the whole harmonic group, the mitigation of the harmonic distortion is performed in the complete harmonic range as it is clearly shown in Fig. 12f. In addition, as expected observing Fig. 5b and Fig. 6b, the resulting harmonic magnitude of the whole second group remains unaltered while the third harmonic group slightly increases.

The same experiment has been performed in order to evaluate the impact of the modulation techniques in the operation of the PMSM in terms of the phase currents quality. The experimental results are summarized in Fig. 13, where the three-phase currents as well as the harmonic spectrum of the phase *a* have been plotted applying the three PWM methods for comparison purposes. As it can be observed, considering the proposed adaptive multi-carrier PWM technique, the phase currents experience an increase of the harmonic distortion, similarly to that present in the result obtained applying the tri-carrier PWM method with fixed displacement angles. More particularly, the normalized THD of i_a (calculated up to 17kHz) applying all modulation techniques are 3.55% (traditional single-carrier PWM), 6.27% (tri-carrier PWM with fixed displacement angles) and 6.02% with the proposed method. However, it has to be noticed that according with Fig 13b, Fig 13d and Fig. 13f, the magnitude of the distortion in the three-phase currents is quite limited since they are in the range of miliamperes.

The previous experiments have been also performed considering different rotation speed values of the PMSM. A comparison between the resulting CMV as well as i_a quality is reported in Table 2, where the THD has been calculated up to 17kHz. It can be observed that the advantages of the proposed method remain.

From these results, it can be concluded that the proposed adaptive multi-carrier modulation technique has a significant positive impact mitigating the CMV harmonic content. In addition, the resulting degradation in the three-phase currents highly depends on the machine's inductance. This inductance is the result of multiple factors such as mechanical requirements as well as the voltage/current ratings, among
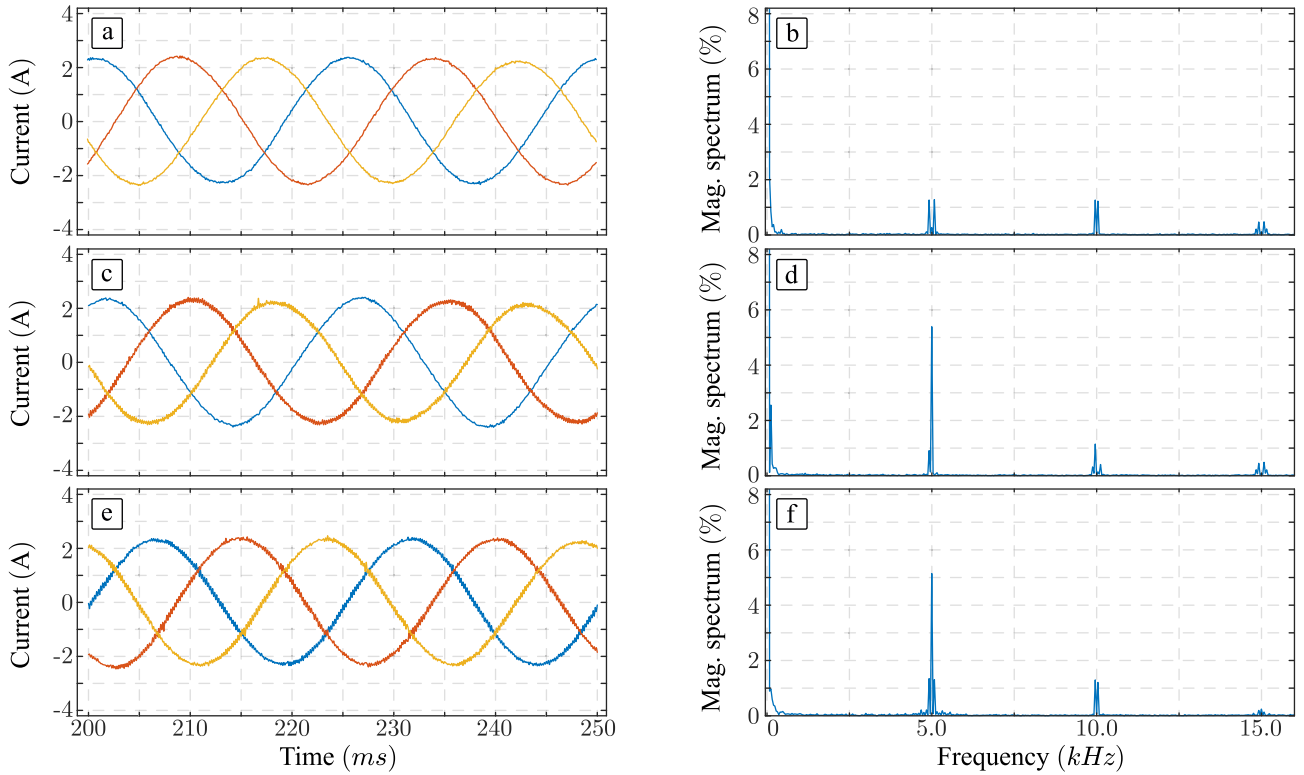
FIGURE 13. Phase currents (left) and phase *a* current THD (right) using a) and b) the traditional single-carrier PWM method c) and d) the tri-carrier PWM with fixed displacement angles [35] e) and f) using the adaptive multi-carrier PWM technique.

TABLE 2. Normalized CMV THD and phase current THD of the phase *a* considering up to 17kHz using the traditional single-carrier PWM, the fixed carrier phase-displacement angle tri-carrier PWM method [35] and the proposed adaptive multi-carrier PWM technique.

Speed [rpm]	ma [p.u.]	CMV *THD* [%]			i_a *THD* [%]		
		single-carrier	multi-carrier [35]	adaptive multi-carrier	single-carrier	multi-carrier [35]	adaptive multi-carrier
400	0.53	107.24	38.42	35.04	2.80	7.55	7.82
600	0.75	90.46	42.52	38.04	3.55	6.27	6.02
800	0.98	71.24	39.44	39.12	3.35	4.23	4.39

others. In conclusion, in many industrial applications the resulting machine's inductance is high and the increase of the current THD can be negligible making this drawback acceptable. This fact confirms that the proposed multi-carrier modulation method is able to mitigate the impact of the power converter operation over the remaining lifetime of the machine.

VI. IMPACT OF THE CMV OVER THE LEAKAGE CURRENT AND THE SHAFT VOLTAGE

As it has been mentioned previously, the presence of a high CMV value accelerates the bearing degradation because of the provoked leakage currents. In this sense, from captured CMV voltages in Fig. 12, the impact over the leakage current as well as the shaft voltage has been determined using a specialized simulation environment considering the parasitic model shown in Fig. 14.

Parameter values	
$R_s = 0.3\,\Omega$	$C_b = 590pF$
$R_p = 10k\Omega$	$C_{rf} = 1.66nF$
$L = 2.18mH$	$C_{wf} = 3nF$
$L_g = 10\mu H$	$C_{wr} = 1pF$
$R_g = 0.1\,\Omega$	$C_g = 4nF$
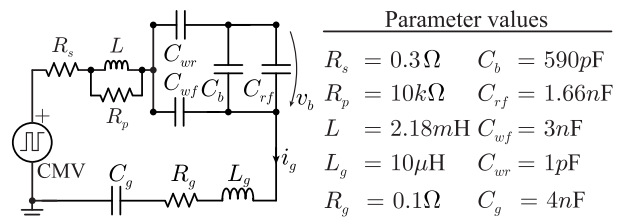
FIGURE 14. Circuit parameters of the experimental setup model.

This model has been realized following the work presented in [21]. The common mode circuit of the machine winding consists of inductive (L) and resistive (R_s) components due to the stator's inductance and resistance. Also the parallel parasitic resistance of the winding (due to insulation) is considered with a lumped resistor R_p.

From the windings to the frame there are two capacitive paths: the first, represented by C_{wf}, is the capacitance

FIGURE 15. PMSM shaft voltage (left) and leakage current (right) using a) and b) the traditional single-carrier PWM method c) and d) tri-carrier PWM [35] e) and f) proposed adaptive multi-carrier PWM method.

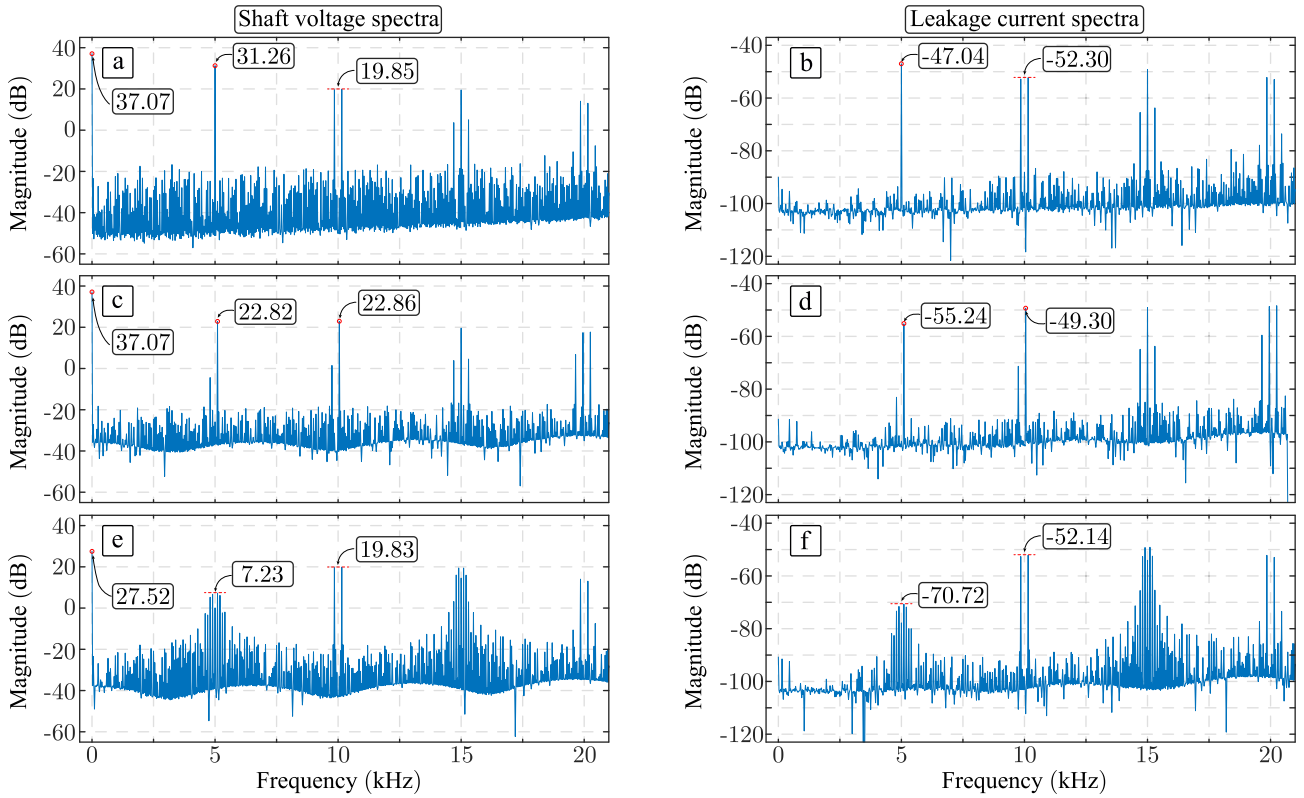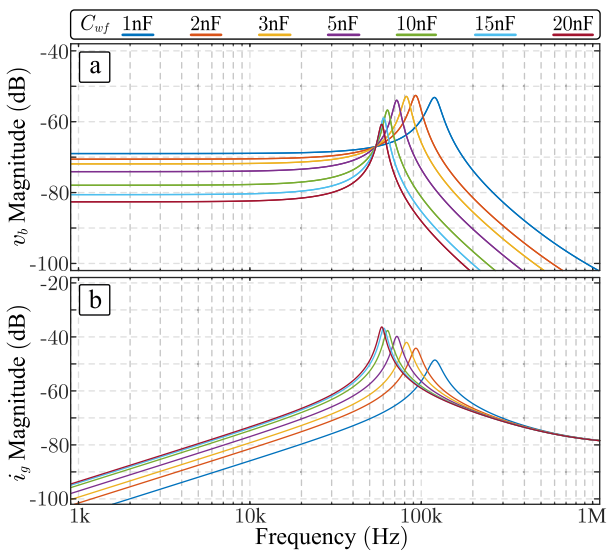**FIGURE 16.** Frequency response of the bearing voltage v_b and leakage current i_g depending on the value of C_{wf}.

between the windings and the frame, the second path closes through the rotor. C_{wr} is the capacitance between the winding and the rotor. The voltage across the rotor and the frame is the so-called shaft voltage and it is an important indicator for the bearings reliability. Also, some capacitive components can be found: C_{rf} is the capacitance between rotor and the

frame and C_b is the capacitance due to the bearings. The current that flows through this capacitance is responsible for the bearing degradation. The other parameters regards to the ground connection: R_g and L_g are resistance and inductance of the path connecting the frame of the machine to ground of the converter and C_g represents the high-voltage capacitors that are usually connected between the DC-link of the converter and ground. The value of the parameters can change depending on the machine type (a reduced air-gap, for example, reduces the C_{wf}), however it is fulfilled that a reduced CMV excitation reduces the current through C_b.

On one hand, it is possible to determine the provoked shaft voltage in the PMSM by the application of different modulation techniques. Firstly, after the application of the fixed-angles tri-carrier modulation method [35], the main harmonic component located at $[m = 1, n = 0]$ is effectively eliminated whereas a new harmonic component located at $[m = 1, n = 2]$ (with an amplitude approximately 3dB lower) appears as it is expected. Additionally, the corresponding dc component remain constant whereas second harmonic group increases (with an amplitude 3dB higher). These results can be consulted in Fig. 15a and 15c. However, considering the proposed modulation technique, as it can be observed in Fig. 15e, the resulting harmonic magnitude in the first group as well as the dc component suffer a great reduction while the second harmonic group remains unaltered. In addition, the leakage current has been also represented and similar

positive conclusions can be obtained from Fig. 15. In addition, in order to consider the possible resonances in the bearing voltage and the leakage current, the frequency response of the system depending on the value of C_{wf} has been studied. The obtained results are shown in Fig. 16 where it can be seen that the resonances are always located at high frequencies, not affecting the expected performance.

VII. CONCLUSION

Leakage currents are responsible in electric drives, among others, of the degradation of the motor bearing reducing its lifetime. In this paper a simple modulation technique to reduce the common-mode voltage of the machine (which causes the leakage current) is proposed. This modulation method is based on the use of a triangular carrier per phase of the power converter and the modification, each sampling time, of the displacement angles between the carriers. The displacement angles calculation is very simple computationally and is based on the minimization of the CMV harmonic content at the carrier frequency via the Fourier expansion series. Each sampling-time, a simple iterative process selects the most convenient phase angle displacements of the carriers to achieve the CMV harmonic mitigation without the introduction of extra hardware components in the system. The effectiveness of the proposed method is proven experimentally and it shows a very promising 50% reduction of the leakage current at the expense of an acceptable increase of the phase currents THD.

REFERENCES

[1] B. K. Bose, "Global energy scenario and impact of power electronics in 21st century," *IEEE Trans. Ind. Electron.*, vol. 60, no. 7, pp. 2638–2651, Jul. 2013.

[2] G. Buticchi, S. Bozhko, M. Liserre, P. Wheeler, and K. Al-Haddad, "On-board microgrids for the more electric aircraft—Technology review," *IEEE Trans. Ind. Electron.*, vol. 66, no. 7, pp. 5588–5599, Jul. 2019.

[3] A. Bindra, "Wide-bandgap-based power devices: Reshaping the power electronics landscape," *IEEE Power Electron. Mag.*, vol. 2, no. 1, pp. 42–47, Mar. 2015.

[4] D. G. Holmes and T. A. Lipo. 2003. *Wiley-IEEE Press*. [Online]. Available: https://ieeexplore.ieee.org/xpl/articleDetails.jsp?arnumber=5311953

[5] A. Yazdani and R. Iravani, *Voltage-Sourced Converters in Power Systems: Modeling, Control, and Applications.* Hoboken, NJ, USA: Wiley, 2010.

[6] J. I. Leon, S. Kouro, L. G. Franquelo, J. Rodriguez, and B. Wu, "The essential role and the continuous evolution of modulation techniques for voltage-source inverters in the past, present, and future power electronics," *IEEE Trans. Ind. Electron.*, vol. 63, no. 5, pp. 2688–2701, May 2016.

[7] J. I. Leon, S. Vazquez, and L. G. Franquelo, "Multilevel converters: Control and modulation techniques for their operation and industrial applications," *Proc. IEEE*, vol. 105, no. 11, pp. 2066–2081, Nov. 2017.

[8] S. Vazquez, J. Rodriguez, M. Rivera, L. G. Franquelo, and M. Norambuena, "Model predictive control for power converters and drives: Advances and trends," *IEEE Trans. Ind. Electron.*, vol. 64, no. 2, pp. 935–947, Feb. 2017.

[9] B. M. Wilamowski and J. D. Irwin, *Power Electronics and Motor Drives.* Boca Raton, FL, USA: CRC Press, 2017.

[10] D. Eaton, J. Rama, and P. Hammond, "Neutral shift [five years of continuous operation with adjustable frequency drives]," *IEEE Ind. Appl. Mag.*, vol. 9, no. 6, pp. 40–49, Nov. 2003.

[11] J. Kalaiselvi and S. Srinivas, "Bearing currents and shaft voltage reduction in dual-inverter-fed open-end winding induction motor with reduced CMV PWM methods," *IEEE Trans. Ind. Electron.*, vol. 62, no. 1, pp. 144–152, Jan. 2015.

[12] A. Mütze, "Thousands of hits: On inverter-induced bearing currents, related work, and the literature," *Elektrotechnik und Informationstechnik*, vol. 128, nos. 11–12, pp. 382–388, Dec. 2011.

[13] G. L. Skibinski, R. J. Kerkman, and D. Schlegel, "EMI emissions of modern PWM AC drives," *IEEE Ind. Appl. Mag.*, vol. 5, no. 6, pp. 47–80, Nov. 1999.

[14] Y. Isomura, K. Yamamoto, S. Morimoto, T. Maetani, A. Watanabe, and K. Nakano, "Study of the further reduction of shaft voltage of brushless DC motor with insulated rotor driven by PWM inverter," *IEEE Trans. Ind. Appl.*, vol. 50, no. 6, pp. 3738–3743, Nov. 2014.

[15] D. Jiang, J. Chen, and Z. Shen, "Common mode EMI reduction through PWM methods for three-phase motor controller," *CES Trans. Electr. Mach. Syst.*, vol. 3, no. 2, pp. 133–142, Jun. 2019.

[16] S.-T. Lee, J.-K. Park, C.-L. Jeong, S.-H. Rhyu, and J. Hur, "Shaft-to-frame voltage mitigation method by changing winding-to-rotor parasitic capacitance of IPMSM," *IEEE Trans. Ind. Appl.*, vol. 55, no. 2, pp. 1430–1436, Mar. 2019.

[17] Y. Han, H. Lu, Y. Li, and J. Chai, "Analysis and suppression of shaft voltage in SiC-based inverter for electric vehicle applications," *IEEE Trans. Power Electron.*, vol. 34, no. 7, pp. 6276–6285, Jul. 2019.

[18] A. M. Hava and E. Ün, "A high-performance PWM algorithm for common-mode voltage reduction in three-phase voltage source inverters," *IEEE Trans. Power Electron.*, vol. 26, no. 7, pp. 1998–2008, Jul. 2011.

[19] B. Muralidhara, A. Ramachandran, R. Srinivasan, and M. C. Reddy, "Experimental measurement of shaft voltage and bearing current in an inverter fed three phase induction motor drive," in *Proc. 3rd Int. Conf. Electron. Comput. Technol.*, vol. 2, Apr. 2011, pp. 37–41.

[20] J. Song-Manguelle, S. Schroder, T. Geyer, G. Ekemb, and J.-M. Nyobe-Yome, "Prediction of mechanical shaft failures due to pulsating torques of variable-frequency drives," *IEEE Trans. Ind. Appl.*, vol. 46, no. 5, pp. 1979–1988, Sep. 2010.

[21] O. Magdun and A. Binder, "High-frequency induction machine modeling for common mode current and bearing voltage calculation," *IEEE Trans. Ind. Appl.*, vol. 50, no. 3, pp. 1780–1790, May 2014.

[22] H. M. Flieh, E. Totoki, and R. D. Lorenz, "Dynamic shaft torque observer structure enabling accurate dynamometer transient loss measurements," *IEEE Trans. Ind. Appl.*, vol. 54, no. 6, pp. 6121–6132, Nov. 2018.

[23] R. Naik, T. A. Nondahl, M. J. Melfi, R. Schiferl, and J.-S. Wang, "Circuit model for shaft voltage prediction in induction motors fed by PWM-based AC drives," *IEEE Trans. Ind. Appl.*, vol. 39, no. 5, pp. 1294–1299, Sep. 2003.

[24] D. Han, C. T. Morris, and B. Sarlioglu, "Common-mode voltage cancellation in PWM motor drives with balanced inverter topology," *IEEE Trans. Ind. Electron.*, vol. 64, no. 4, pp. 2683–2688, Apr. 2017.

[25] N.-S. Choi, E.-C. Lee, and K.-S. Ahn, "Space vector PWM for common mode voltage reduction and neutral point voltage balancing in three-level converters," in *Proc. IEEE 8th Int. Power Electron. Motion Control Conf. (IPEMC-ECCE Asia)*, May 2016, pp. 2401–2405.

[26] C. Choochuan, "A survey of output filter topologies to minimize the impact of PWM inverter waveforms on three-phase AC induction motors," in *Proc. Int. Power Eng. Conf.*, May 2005, pp. 1–544.

[27] C. Mei, J. C. Balda, and W. P. Waite, "Cancellation of common-mode voltages for induction motor drives using active method," *IEEE Trans. Energy Convers.*, vol. 21, no. 2, pp. 380–386, Jun. 2006.

[28] M. C. D. Piazza, G. Tine, and G. Vitale, "An improved active common-mode voltage compensation device for induction motor drives," *IEEE Trans. Ind. Electron.*, vol. 55, no. 4, pp. 1823–1834, Apr. 2008.

[29] F. Fan, K. Y. See, J. K. Banda, X. Liu, and A. K. Gupta, "Investigation and mitigation of premature bearing degradation in motor drive system," *IEEE Electromagn. Compat. Mag.*, vol. 8, no. 1, pp. 75–81, Apr. 2019.

[30] K. Jayaraman and M. Kumar, "Design of passive common-mode attenuation methods for inverter-fed induction motor drive with reduced common-mode voltage PWM technique," *IEEE Trans. Power Electron.*, vol. 35, no. 3, pp. 2861–2870, Mar. 2020.

[31] R. M. Tallam, R. J. Kerkman, D. Leggate, and R. A. Lukaszewski, "Common-mode voltage reduction PWM algorithm for AC drives," *IEEE Trans. Ind. Appl.*, vol. 46, no. 5, pp. 1959–1969, Sep. 2010.

[32] M. Cacciato, A. Consoli, G. Scarcella, and A. Testa, "Reduction of common-mode currents in PWM inverter motor drives," *IEEE Trans. Ind. Appl.*, vol. 35, no. 2, pp. 469–476, Mar. 1999.

[33] J. Adabi, A. Ghosh, A. Nami, A. A. Boora, F. Zare, and F. Blaabjerg, "Common-mode voltage reduction in a motor drive system with a power factor correction," *IET Power Electron.*, vol. 5, no. 3, pp. 366–375, Mar. 2012.

[34] J. Espina, C. Ortega, L. de Lillo, L. Empringham, J. Balcells, and A. Arias, "Reduction of output common mode voltage using a novel SVM implementation in matrix converters for improved motor lifetime," *IEEE Trans. Ind. Electron.*, vol. 61, no. 11, pp. 5903–5911, Nov. 2014.

[35] J. W. Kimball and M. Zawodniok, "Reducing common-mode voltage in three-phase sine-triangle PWM with interleaved carriers," *IEEE Trans. Power Electron.*, vol. 26, no. 8, pp. 2229–2236, Aug. 2011.

[36] D. G. Holmes, "A general analytical method for determining the theoretical harmonic components of carrier based PWM strategies," in *Proc. IEEE Ind. Appl. Conf. 33rd IAS Annu. Meeting*, vol. 2, Oct. 1998, pp. 1207–1214.

[37] A. Marquez, J. I. Leon, S. Vazquez, R. Portillo, L. G. Franquelo, E. Freire, and S. Kouro, "Variable-angle phase-shifted PWM for multilevel three-cell cascaded H-bridge converters," *IEEE Trans. Ind. Electron.*, vol. 64, no. 5, pp. 3619–3628, May 2017.

[38] A. Marquez, V. G. Monopoli, J. I. Leon, Y. Ko, G. Buticchi, S. Vazquez, M. Liserre, and L. G. Franquelo, "Sampling-time harmonic control for cascaded H-bridge converters with thermal control," *IEEE Trans. Ind. Electron.*, vol. 67, no. 4, pp. 2776–2785, Apr. 2020.

[39] *Plexim RT Box Rapid Prototype Platform.* Accessed: Jan. 14, 2021. [Online]. Available: https://www.plexim.com/

[40] B. Zheng, Y. Xu, G. Wang, G. Yu, H. Yan, M. Wang, and J. Zou, "Carrier frequency harmonic suppression in dual three-phase permanent magnet synchronous motor system," *IET Electr. Power Appl.*, vol. 13, no. 11, pp. 1763–1772, May 2019.

JOSE I. LEON (Fellow, IEEE) was born in Cadiz, Spain. He received the B.S., M.S., and Ph.D. degrees in telecommunications engineering from the Universidad de Sevilla (US), Seville, Spain, in 1999, 2001, and 2006, respectively.

He is currently an Associate Professor with the Department of Electronic Engineering, US. Since 2019, he has been the Chair Professor with the Department of Control Science and Engineering, Harbin Institute of Technology, China. His research interest includes modulation and control of power converters for high-power applications and renewable energy systems. In 2017, he was elevated to the IEEE fellow grade with the following citation "for contributions to high-power electronic converters." He was a co-recipient of the 2008 Best Paper Award of *IEEE Industrial Electronics Magazine*, the 2012 Best Paper Award of the IEEE Transactions on Industrial Electronics, the 2015 Best Paper Award of *IEEE Industrial Electronics Magazine*, the 2014 IEEE J. David Irwin Industrial Electronics Society Early Career Award, the 2017 IEEE Bimal K. Bose Energy Systems Award, and the 2017 Manuel Losada Villasante Award for excellence in research and innovation.

ABRAHAM MARQUEZ ALCAIDE (Member, IEEE) was born in Huelva, Spain, in 1985. He received the B.S., M.S., and Ph.D. degrees in telecommunications engineering from the Universidad de Sevilla (US), Seville, Spain, in 2014, 2016 and 2019, respectively.

His main research interests include modulation techniques, multilevel converters, model-based predictive control of power converters and drives, renewable energy sources, and power devices lifetime extension.

Dr. Marquez was a recipient of the 2015 Best Paper Award of the *IEEE Industrial Electronics Magazine*, as a coauthor.

RAMON PORTILLO (Member, IEEE) was born in Sevilla, Spain. He received the M.Sc. and Ph.D. degrees in electrical engineering from the Universidad de Sevilla, Seville, in 2003 and 2012, respectively.

Since 2003, he has been an Assistant Professor with the Department of Electronic Engineering, Universidad de Sevilla. His research interests include power electronic systems, modulation and control of power electronic converters, renewable energy applications, and aerospace power electronics applications.

Dr. Portillo was a recipient of the 2008 Best Paper Award of the *IEEE Industrial Electronics Magazine*, as a coauthor, and the 2012 Best Paper Award of the IEEE Transactions on Industrial Electronics.

HAO YAN (Member, IEEE) received the B.S., M.S., and Ph.D. degrees in electrical engineering from the Harbin Institute of Technology, Harbin, China, in 2011, 2013 and 2018, respectively.

From 2017 to 2019, he was with the Power Electronics, Machines and Control Group, University of Nottingham, Ningbo, China, and worked on power electronics for electrical drives. From 2019 to 2020, he was a Research Fellow with the Rolls-Royce@NTU Corporate Lab, Nanyang Technological University, Singapore. He is currently an Associate Professor with the School of Civil Aviation, Northwestern Polytechnical University, Xi'an, China. His current research interests include permanent-magnet machine drives and power converters in more electric aircraft.

XUCHEN WANG (Student Member, IEEE) was born in Taizhou, China, in 1993. She received the B.Eng. degree (Hons.) in electrical and electronic engineering and the Ph.D. degree in electrical engineering from the University of Nottingham, Ningbo, China, in 2015 and 2019, respectively.

She is currently a Researcher with the Department of Electrical and Electronic Engineering (PEMC group), University of Nottingham. Her research interest includes design, modeling, and control of multiphase drives.

GIAMPAOLO BUTICCHI (Senior Member, IEEE) received the master's degree in electronic engineering and the Ph.D. degree in information technologies from the University of Parma, Italy, in 2009 and 2013, respectively.

In 2012, he was a Visiting Researcher with the University of Nottingham, U.K. From 2014 to 2017, he was a Postdoctoral Researcher and a Guest Professor with the University of Kiel, Germany. In 2017, he was appointed as an Associate Professor in electrical engineering with the University of Nottingham, Ningbo, China, and the Head of power electronics with the Nottingham Electrification Center. In 2020, he was promoted to a Professor. He is currently one of the advocates for DC distribution systems and multi-port power electronics onboard the future aircraft. He is the author/coauthor of more than 210 scientific articles. His research interests include power electronics for renewable energy systems, smart transformer fed micro-grids, and dc grids for the more electric aircraft.

Dr. Buticchi was awarded the Von Humboldt Postdoctoral Fellowship, to carry out research related to fault tolerant topologies of smart transformers, during his stay in Germany. He is currently the Chair of the IEEE Industrial Electronics Society Technical Committee on Renewable Energy Systems. He is also an Associate Editor of the IEEE Transactions on Industrial Electronics, the IEEE Transactions on Transportation Electrification, and the IEEE Open Journal of the Industrial Electronics Society.

SERGIO VAZQUEZ (Fellow, IEEE) was born in Seville, Spain, in 1974. He received the M.S. and Ph.D. degrees in industrial engineering from the University of Seville (US), in 2006 and 2010, respectively.

Since 2002, he has been with the Power Electronics Group, working in research and development projects. He is currently an Associate Professor with the Department of Electronic Engineering, US. His research interests include power electronics systems and modeling, modulation, and control of power electronics converters applied to renewable energy technologies.

Dr. Vazquez was a recipient of the 2012 Best Paper Award of the IEEE TRANSACTIONS ON INDUSTRIAL ELECTRONICS, as a coauthor, and the 2015 Best Paper Award of the *IEEE Industrial Electronics Magazine*. He is also involved in the Energy Storage Technical Committee of the IEEE Industrial Electronics Society and serving as an Associate Editor of the IEEE TRANSACTIONS ON INDUSTRIAL ELECTRONICS.

contributions to grid connection of renewable energy systems and industrial drives." He has been awarded with the ERC Consolidator Grant for the project The Highly Efficient And Reliable smart Transformer (HEART), a new Heart for the Electric Distribution System. He has received the IES 2009 Early Career Award, the IES 2011 Anthony J. Hornfeck Service Award, the 2014 Dr. Bimal Bose Energy Systems Award, the 2011 Industrial Electronics Magazine Best Paper Award, and the Third Prize Paper Award by the Industrial Power Converter Committee at ECCE 2012. He is also an Associate Editor of the IEEE TRANSACTIONS ON INDUSTRIAL ELECTRONICS, *IEEE Industrial Electronics Magazine*, and IEEE TRANSACTIONS ON INDUSTRIAL INFORMATICS, and the Co-Editor-in-Chief of IEEE TRANSACTIONS ON POWER ELECTRONICS, and IEEE JOURNAL OF EMERGING AND SELECTED TOPICS IN POWER ELECTRONICS. He has been the Founder and the Editor-in-Chief of the *IEEE Industrial Electronics Magazine*, the Founder and the Chairman of the Technical Committee on Renewable Energy Systems, the Co-Chairman of the International Symposium on Industrial Electronics (ISIE 2010), and the IES Vice-President responsible of the publications.

VITO GIUSEPPE MONOPOLI (Senior Member, IEEE) received the M.Sc. and Ph.D. degrees in electrical engineering from Bari Polytechnic, Bari, Italy, in 2000 and 2004, respectively. He is currently an Assistant Professor with Bari Polytechnic. His research interests include multilevel converters and the analysis of harmonic distortion produced by power converters and electrical drives. He is particularly interested in innovative control techniques for power converters. He is also a member of the IEEE Industry Applications Society, the IEEE Industrial Electronics Society, and the IEEE Power Electronics Society.

LEOPOLDO G. FRANQUELO (Life Fellow, IEEE) was born in Málaga, Spain. He received the M.Sc. and Ph.D. degrees in electrical engineering from the Universidad de Sevilla, Seville, Spain, in 1977 and 1980, respectively.

From 1982 to 1986, he was an Associate Professor with the Department of Electronics Engineering, Sevilla University, where he has been a Professor, since 1986. Since 2016, he has been a 1000 Talent Professor with the Department of Control Science and Engineering, Harbin Institute of Technology. He has participated in more than 100 industrial and research and development projects and has published more than 300 articles, 76 of them in IEEE journals. His current research interests include modulation techniques for multilevel inverters and application to power electronic systems for renewable energy systems.

Dr. Franquelo was a Member-at-Large of the IES AdCom from 2002 to 2003, the vice president for conferences from 2004 to 2007, the President Elect of the IES from 2008 to 2009, the President of the IES from 2010 to 2011. He is also an IES AdCom Life Member. He received the prestigious Andalusian Research Award and the FAMA Award, recognizing the excellence of his research career, in 2009 and 2013. He has received a number of best paper awards from IEEE journals. He was a recipient of the Eugene Mittelmann Outstanding Research Achievement Award in 2012 and the Antohny J. Hornfeck Service Award from IEEE-IES in 2015. He became an Associate Editor in 2007, the Co-Editor-in-Chief in 2014, and has been the Editor-in-Chief since 2016 of IEEE TRANSACTIONS ON INDUSTRIAL ELECTRONICS. Since 2006, he has been an IEEE Industrial Electronics Society (IES) Distinguished Lecturer.

MARCO LISERRE (Fellow, IEEE) received the M.Sc. and Ph.D. degrees in electrical engineering from Bari Polytechnic, in 1998 and 2002, respectively. He has been an Associate Professor with Bari Polytechnic and a Professor in reliable power electronics with Aalborg University, Denmark. He is currently a Full Professor and the Chair of power electronics with the Christian-Albrechts-University of Kiel, Germany. He has published over 300 technical articles (more than 100 of them in international peer-reviewed journals), four chapters of a book and a book *Grid Converters for Photovoltaic and Wind Power Systems* (IEEE-Wiley), a second reprint, also translated in Chinese. These works have received more than 20000 citations. He is listed in ISI Thomson report "The world's most influential scientific minds" from 2014. He is also a member of IAS, PELS, PES, and IES, and a senior member of IES AdCom. In 2013, he was elevated to the IEEE fellow grade with the following citation "for

● ● ●